Multipulse Operation and Optical Detection of Nuclear Spin Coherence in a GaAs/AlGaAs Quantum Well

Y. Kondo, ^{1,*} M. Ono, ¹ S. Matsuzaka, ^{1,2} K. Morita, ^{2,1,†} H. Sanada, ^{1,‡} Y. Ohno, ^{1,§} and H. Ohno ^{1,2,||}

¹Laboratory for Nanoelectronics and Spintronics, Research Institute of Electrical Communication, Tohoku University, Katahira 2-1-1, Aoba-ku, Sendai 980-8577, Japan

²ERATO Semiconductor Spintronics Project, Japan Science and Technology Agency, Japan (Received 6 July 2008; published 14 November 2008)

We demonstrate manipulation of nuclear spin coherence in a GaAs/AlGaAs quantum well by optically detected nuclear magnetic resonance (NMR). A phase shift of the Larmor precession of photoexcited electron spins is detected to read out the hyperfine-coupled nuclear spin polarization. Multipulse NMR sequences are generated to control the population and examine the phase coherence in quadrupolar-split spin-3/2 ⁷⁵As nuclei. The phase coherence among the multilevel nuclear spin states is addressed by application of pulse sequences that are used in quantum gate operations.

DOI: 10.1103/PhysRevLett.101.207601 PACS numbers: 76.70.Hb, 78.47.jc, 78.66.Fd

A new class of nuclear magnetic resonance (NMR) [1] with high sensitivity and high spatial resolution has become an important tool to investigate intriguing spinrelated physics in semiconductor nanostructures [2], in which one can control the interaction between electron and nuclear spins by electrical and optical means [3–8]. In GaAs, which has been extensively studied in the research field of semiconductor spintronics and is widely utilized in electronic and optical devices, the degree of nuclear polarization can be increased by orders of magnitude via contact hyperfine interaction with nonequilibrium electron spin systems. These can be achieved in such electronic systems as specific fractional [3] and integer quantum Hall edge states [4], and by irradiation of circularly polarized light [9]. In both electrical and optical approaches, nuclear spin dynamics can also be detected sensitively by measuring the change of resistance [3,4], and magneto-optical effect [5-8] or luminescence polarization [10], respectively. In our previous work, we have developed a time-resolved optical magnetometry to read out the coherent dynamics of nuclear polarization [11], in which spin precession of electrons monitors the nuclear polarization via hyperfine interaction. This allows us to sensitively detect transient polarization of the small number of nuclear spins that contains multiple spin levels without defining any specific device geometry and recombination process with holes that enhance spin relaxation via exchange interaction.

In GaAs, all the constituent atoms, 69 Ga, 71 Ga, and 75 As, have nuclear spin I=3/2. Coherent dynamics of small ensemble of the nuclear spins (less than the detection limit of conventional NMR technique) have recently been studied in GaAs-based devices, where hyperfine-coupled electrons are well confined [3,4,12]. In those experiments, phase coherence of the nuclear spins has been addressed from the analysis of Rabi oscillation and spin-echo experiments. It is intriguing to extend the range of manipulation

of nuclear spin states to manifest the coherent features of quadrupolar-split nuclear spins in GaAs. In this Letter, we show the manipulation of the phase coherence in nuclear spin ensemble in a GaAs/AlGaAs single quantum well (QW) by employing a multipulse sequence that is identical to the quantum gate operation for preparation of superposition as well as the Bell states of (virtual) 2-qubit states, i.e., Hadmard (H-) and controlled-NOT (CNOT) gates based on classical rf-pulse NMR technique [12,13].

The sample studied here is a single, 8.5 nm-wide $GaAs/A_{0.3}Ga_{0.7}As$ QW with 5×10^{17} cm⁻³ Si donor concentration. The structure was grown on (110) GaAs substrate by molecular beam epitaxy. In n-type (110) GaAs QWs, the typical spin coherence time of electrons is extended to several nanoseconds at low temperatures, an order of magnitude longer than that of (001) GaAs QWs [8]. This enhances dynamic nuclear polarization via contact hyperfine coupling with optically excited spins. Because the spin lifetime is long, the Larmor precession of photoexcited electron spins can also be used as a sensitive probe of nuclear polarization that can be traced by a time-resolved Faraday rotation (TRFR) technique [7,8]. For transmission measurements, the GaAs substrate was removed by selective etching with the epilayer glued on fused silica glass. This introduces mechanical strain and noncentrosymmetric electric field in the QW, resulting in quadrupolar splitting of I = 3/2 nuclear spins.

When a static magnetic field B_0 is applied (in the z direction), nuclear spin states (with spin-angular momentum I) are described by the Hamiltonian $H_0 = -\hbar\omega_0I_z + \hbar\omega_Q(3I_z^2 - I^2)$, where $\hbar\omega_0 = \gamma_N\hbar B_0$ is the Zeeman energy, $\hbar\omega_Q$ the quadrupolar splitting as shown in Fig. 1(a), \hbar the reduced Planck constant, and γ_N the gyromagnetic ratio of the nuclei. The phase in I = 3/2 nuclear spins can be controlled by applying rf magnetic field $B_{\rm rf}$ so that the total Hamiltonian is given by $H = H_0 - \gamma_N\hbar B_{\rm rf}(I_x\cos\varphi + I_y\sin\varphi)$, where φ corresponds to the

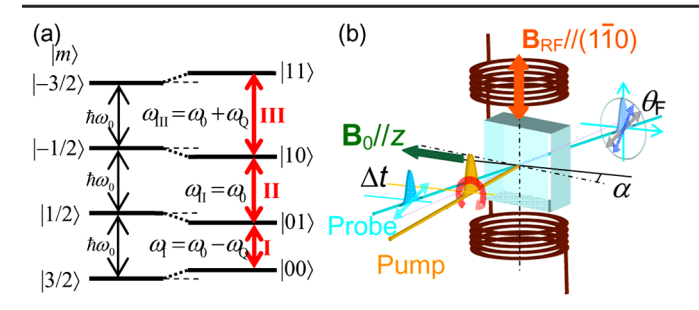


FIG. 1 (color online). (a) Energy level diagram of quadrupolar-split I=3/2 nuclear spin states $|m\rangle$. ω_0 is the Zeeman gap and ω_Q is the quadrupolar splitting. (b) The experimental setup of the TRFR experiments. The (110) GaAs/AlGaAs QW was set so that the [001] crystalline axis in the QW plane was tilted about 2° from $B_0//z$.

phase in the *x-y* plane. In order to describe the manipulation of nuclear spin states by phase-controlled multi pulse sequences, we utilized the terminology in quantum information processing in the remainder of this Letter: The eigenstates of H_0 , i.e., $|m\rangle = |-3/2\rangle$, $|-1/2\rangle$, $|+1/2\rangle$, and $|+3/2\rangle$, are taken as basis of virtual two-qubit system $|11\rangle$, $|10\rangle$, $|01\rangle$, and $|00\rangle$.

The setup for optical NMR detection is schematically shown in Fig. 1(b). The sample is placed in a magnetooptical cryostat with superconducting magnet (Oxford Instruments SM-7/8T), where B_0 is applied perpendicular to the optical axis: The (110) QW plane is tilted by a small angle ($\alpha \sim 2^{\circ}$ between the [001] crystalline axis and B_0 . A hand-made split coil is placed near the sample to apply B_{rf} along [110] axis. Rf pulses were generated by a programmable function generator. The amplified rf power was fed to the LC resonator which is impedance matched at around 5 MHz. In TRFR measurements, a 3 ps-pulse train was generated by a mode-locked Ti:Sapphire laser at 76 MHz, and the photon energy was tuned to the resonant excitation of the lowest heavy-hole exciton in the OW. A laser pulse was separated into pump (10 mW) and probe (0.6 mW) pulses, and they are focused to overlap onto the sample with a diameter of 50 μ m. The circularly polarized pump excites spin polarized electrons normal to the QW plane, and the Faraday rotation θ_F of the time-delayed (Δt) , linear polarized probe is detected by using a balanced detector. The measurements were done at 2.7–3.7 K.

In the existence of nuclear polarization, the Larmor frequency of electron spins is given by $|\omega_L| = |\hat{g}\mu_B B_0 + \sum_j A_{Hj} \text{tr}(\boldsymbol{\rho}_j \boldsymbol{I}_z) \cdot \boldsymbol{z}|/\hbar$, where \hat{g} is the anisotropic electron g tensor $(g_{[001]} = -0.17 \text{ and } g_{[110]} = -0.22 \text{ for the present sample})$, μ_B the Bohr magneton, A_{Hj} the hyperfine constant, and $\text{tr}(\boldsymbol{\rho}_j \boldsymbol{I}_z)$ is the z component of the nuclear magnetization of the j element $(j = ^{69}\text{Ga}, ^{71}\text{Ga}, \text{ and }^{75}\text{As})$. $\boldsymbol{\rho}_j$ is a 4×4 density matrix for each nuclear species in the basis of $|-3/2\rangle$, $|-1/2\rangle$, $|+1/2\rangle$, and $|+3/2\rangle$ states. The evolution of $\boldsymbol{\rho}_j$ after the application of \boldsymbol{B}_{rf} pulses can

be evaluated by measuring the change of θ_F at fixed Δt (labeled as $\Delta \theta_F$). We set Δt so that $\Delta \theta_F \propto \text{tr}(\boldsymbol{\rho}_i \boldsymbol{I}_z)$ [11].

The inset of Fig. 2 shows the cw-NMR spectrum for ⁷⁵As, i.e., the trace of θ_F as a function of $f_{\rm rf} = \omega_{\rm rf}/2\pi$ under radiation of cw- \boldsymbol{B}_{rf} ($B_0 = 0.723$ T). Three distinct resonance lines are resolved, corresponding to $|+3/2\rangle \leftrightarrow |+1/2\rangle$, (II) $|-1/2\rangle \leftrightarrow |+1/2\rangle$, and (III) $|-3/2\rangle \leftrightarrow |-1/2\rangle$ transitions, respectively, as defined in Fig. 1(a). While similar NMR spectra were obtained for ⁶⁹Ga and ⁷¹Ga, we employed ⁷⁵As as a target nuclei since it has the largest quadrupolar splitting ($\omega_O/2\pi \sim 50 \text{ kHz}$) compared to those of 69 Ga and 71 Ga ($12 \sim 18$ kHz) [14]. As $|B_{\rm rf}|$ is increased, multiple quantum transitions (two- or three-photon absorption) are enhanced (not shown). In the following experiments, we set $|B_{\rm rf}| \sim 1$ mT so that multiple quantum transitions are suppressed to improve the fidelity of phase control in transitions between two adjacent levels.

Figure 2 shows $\Delta\theta_F$ measured as a function of the width τ of a single-square-shaped pulse $\boldsymbol{B}_{\rm rf}$, that corresponds to the evolution of $\langle I_z \rangle \equiv {\rm tr}(\boldsymbol{\rho}_{\rm As}\boldsymbol{I}_z)$ (Rabi oscillation). By fitting with the form $\Delta\theta_F(\tau) \propto \cos(2\pi\nu_{\rm Rabi}\tau)\exp(-\tau/T_{\rm 2Rabi})-1$, we found $T_{\rm 2Rabi}$ of the I and II transitions to be 0.9 and 2.1 ms, respectively. The short $T_{\rm 2Rabi}$ for the transition I (and III) may result from the nonuniformity of the strain field which introduces

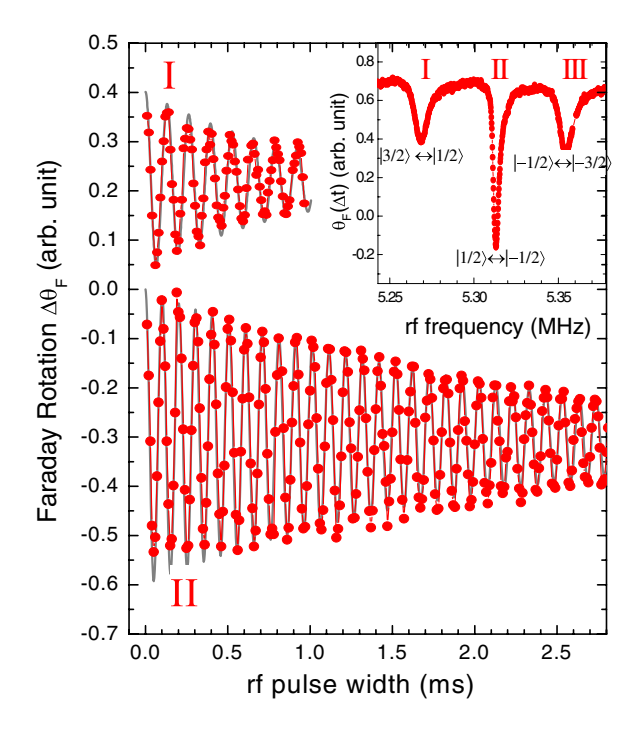


FIG. 2 (color online). Rabi oscillations for I (upper) and II (lower) transitions are shown. $\Delta\theta_F$ reveals the change of the nuclear polarization after application of a single-square $B_{\rm rf}$ pulse. The gray lines are the fitting curves. The decoherence time $T_{\rm 2Rabi}$ for transitions II is 2.1 ms, and that for I is 0.9 ms. The inset is a cw-NMR spectrum of $^{75}{\rm As}$ taken by measuring θ_F at fixed $B_0=0.727$ T and $\Delta t=672$ ps.

broadening of the transition frequencies, while the effect is canceled for transition II in first order perturbation theory [1]. In GaAs OWs, nuclear polarization as high as 20% has been achieved by setting $\alpha \sim 20^{\circ}$ in the TRFR configuration [15]. In the present experiment, however, α was set at 2° in order to cancel out the nuclear dipole-dipole interaction with the first nearest neighbors [1], and the degree of the nuclear polarization is 4–5%. Thus, in the following, we describe the population of ⁷⁵As nuclear spin system by a deviation matrix $\Delta \rho_{As}$, instead of ρ_{As} as defined by $\rho_{\rm As} = 1/4 + \epsilon \Delta \rho_{\rm As}$ with a small number ϵ . We evaluated the population (the diagonal elements of $\Delta \rho_{As}$) by analyzing their NMR spectra, which is obtained after application of a 70 μ s read pulse (close to a π pulse for the range of $\omega_{\rm rf}$) with a 200 μ s interval in order to detect the change in $\langle I_{\tau} \rangle$.

First we examined manipulation of phase in nuclear spin system by phase (φ) -controlled $B_{\rm rf}$ pulses. We measured the φ dependence of $\Delta\theta_F$ after application of successive two $\pi/2$ and π pulses. In Fig. 3, $\Delta\theta_F$ curves for three resonance frequencies are shown when $X(\pi/2) - \varphi(\pi/2)$ and $X(\pi) - \varphi(\pi)$ pulses are applied, respectively, where X represent a pulse with $\varphi = 0^\circ$. We confirmed $\Delta\theta_F \propto \cos\varphi$ for $X(\pi/2) - \varphi(\pi/2)$ and independent of φ for $X(\pi) - \varphi(\pi)$, as expected from the trace on a Bloch sphere.

Starting from the initial population of the nuclear spin states under optical pumping, we generated the pseudopure state (PPS) $|00\rangle_{PPS}$, which is represented by $\Delta \rho_{As}(|00\rangle) = \mathrm{diag}([1/2,1/2,1/2,-3/2])$. $|00\rangle_{PPS}$ is generated by applying two sine-shaped pulses, first 70 μs at ω_{II} and then 45 μs at ω_{III} , slightly modified from the ordinary sequence of a π pulse at ω_{II} and $\pi/2$ pulse at ω_{III} to obtain the target

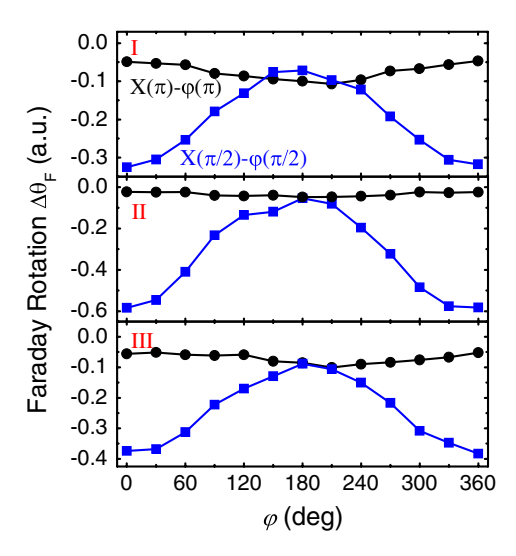


FIG. 3 (color online). Experimental results of the phase control at transitions I, II, and III. $\Delta\theta_F$ is shown as a function of φ after application of $X(\pi/2)_{\text{II}} - \varphi(\pi/2)_{\text{II}}$ (squares) and $X(\pi)_{\text{II}} - \varphi(\pi)_{\text{II}}$ (circles). For each transition, the width of the $\pi/2$ pulse $\sim 70~\mu \text{s}$ was determined from their Rabi oscillations.

 $\Delta \rho_{\rm As}$ [13]. Next we generated a superposition of two states by applying a Hadmard (H-) gate upon the pseudopure state $|00\rangle_{\rm PPS}$, and then the Bell state by applying a CNOT-gate upon the superposition state. For I=3/2 two-qubit spin systems, a H-gate can be constructed by two successive pulses with different phases, a $\pi/2$ pulse at $\omega_{\rm I}$ with $\varphi=90^\circ$ [labeled by $Y(\pi/2)_{\rm I}$] and a π pulse at $\omega_{\rm I}$ with $\varphi=0^\circ$ [labeled by $X(\pi)_{\rm I}$] [13], that turns $|00\rangle$ into a superposition $(|00\rangle+|01\rangle)/\sqrt{2}$. The Bell state $(|00\rangle+|11\rangle)/\sqrt{2}$ is then generated by operating a CNOT-gate, which consists of three π pulses $Y(\pi)_{\rm II}-Y(\pi)_{\rm III}-X(\pi)_{\rm II}$ [13]. These protocols are schematically shown in Fig. 4(a).

In Fig. 4(b), the NMR spectra for the initial pseudopure state (labeled by $|00\rangle_{PPS}$), the superposition ($|00\rangle + |01\rangle$), and the Bell state ($|00\rangle + |11\rangle$) are shown: The baseline of the NMR curve amounts to the averaged nuclear polarization $\langle I_z \rangle$, and the peak and dip in NMR spectra indicate the population difference between two states under resonance at ω_{rf} . For comparison, simulation results of $\langle I_z \rangle$ for each state are plotted in Fig. 4(c) as a function of $\Delta \omega_{rf} = \omega_{rf} - \omega_{II}$. The experimental NMR spectra agree quite well with

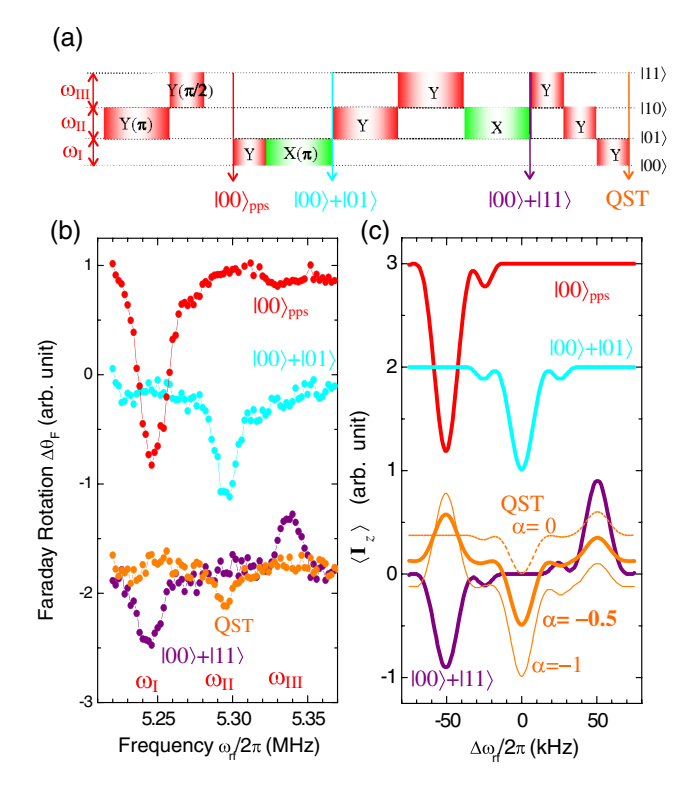


FIG. 4 (color online). (a) The schematic diagram of the multipulse sequence of generation of a pseudopure state $|00\rangle_{PPS}$, a superposition of two states $(|00\rangle + |01\rangle)$, the Bell state $(|00\rangle + |11\rangle)$, and the QST are shown. (b) The experimental NMR spectra for $|00\rangle_{PPS}$, $|00\rangle + |01\rangle$, $|00\rangle + |11\rangle$, and the QST are shown. (c) The simulation results of the NMR spectra for $|00\rangle_{PPS}$, $|00\rangle + |01\rangle$, $|00\rangle + |11\rangle$, and QSTs with the off-diagonal element $\alpha = -1$ (thin solid line), -0.5 (thick solid line), and 0 (thin dotted line), respectively.

the simulations, indicating that the population of each state is controlled by these gate operations.

In order to probe the coherence of the system, we examined the off-diagonal components of $|00\rangle + |11\rangle$, that has the density matrix

$$\Delta \boldsymbol{\rho}_{As}(|00\rangle + |11\rangle = \begin{pmatrix} -0.5 & 0 & 0 & \alpha \\ 0 & 0.5 & 0 & 0 \\ 0 & 0 & 0.5 & 0 \\ \alpha & 0 & 0 & -0.5 \end{pmatrix}$$
(1)

with $\alpha = -1$. If the phase is relaxed, α becomes 0. To detect the off-diagonals by measuring the populations (diagonals), we employed a three-pulse sequence of the quantum state tomography (QST) that is composed of $Y(\pi/2)_{III} - Y(\pi/2)_{II} - Y(\pi/2)_{I}$ [16,17]. The experimental NMR spectrum of the QST is also shown in Fig. 4(b) (labeled by "QST"). For comparison, we calculated the NMR spectra as a function of the off-diagonal value α (-1, -0.5, and 0) and plotted in Fig. 4(c). The position of the baseline $(\langle I_z \rangle)$ and the negative peak at ω_{II} seen in the experimental curve are close to the calculated QST curve with finite phase coherence ($\alpha = -0.5$); in addition, we can also see a small positive peak at $\omega_{\rm I}$ in the experimental QST spectrum. This appears to show that the phase coherence is partially retained after the Hadamard- and CNOT-gate operations, in spite of the fact that the total time of the pulse sequences is 400–500 μ s, which is 1/2–1/4 of $T_{2\text{Rabi}}$ (as shown in Fig. 2) and comparable to the intrinsic spin coherence time $T_2 \sim 600 \, \mu \text{s}$ (370 μs) for transition II (I) obtained by optically detected spin-echo experiments [11,14].

The nuclear spin coherence time in semiconductors can be extended by suppression of nuclear dipole-dipole and/or electron-nuclear spin interactions. In GaAs, it has been demonstrated that the suppression of the hyperfine-interaction by depleting the carrier electrons makes $T_{\rm 2Rabi}$ longer [12]. This can be applied to the optical detection of NMR by using a gated structure [5,6]. The present optical detection scheme is not restricted by the device geometry. We believe that the present optical approach is useful not only for studying phase coherence in quantum states and nuclear spin dependent physics in semiconductor nanostructures but also readout of a quantum information stored in multilevel nuclear spins in dense memory devices [18,19].

We thank K. Ohtani, F. Matsukura, and D. Loss for discussions. This work was partly supported by ERATO and CREST, JST, the Grant-in-Aid for Scientific Research (No. 17686001, and No. 19048007 and No. 19048008 in Priority Area "Creation and control of spin current") from

the Ministry of Education, Culture, Sports, Science, and Technology (MEXT), and the Global COE Program Center of Education and Research for Information Electronics Systems at Tohoku University.

- *Present address: Fujitsu Laboratory Ltd., 10-1 Morinosato-Wakamiya, Atsugi-shi, Kanagawa 243-0197, Japan.
- [†]Present address: Center for Frontier Research of Engineering, Tokushima University, 2-1 Minamijyosanjima-Cho, Tokushima 770-8506, Japan.
- *Present address: NTT Basic Research Laboratories, NTT Corporation, 3-1 Morinosato-Wakamiya, Atsugi 243-0198, Japan.
- §oono@riec.tohoku.ac.jp
- ohno@riec.tohoku.ac.jp
- [1] A. Abragam, *The Principle of Nuclear Magnetism* (Oxford University Press, Oxford, 1961).
- [2] Semiconductor Spintronics and Quantum Computation, edited by D.D. Awschalom, D. Loss, and N. Samarth (Springer, Berlin, 2002).
- [3] G. Yusa et al., Nature (London) 434, 1001 (2005); T. Ota et al., Appl. Phys. Lett. 91, 193101 (2007).
- [4] T. Machida, T. Yamazaki, K. Ikushima, and S. Komiyama, Appl. Phys. Lett. 82, 409 (2003); T. Takahashi *et al.*, *ibid*. 91, 092120 (2007).
- [5] M. Poggio et al., Phys. Rev. Lett. 91, 207602 (2003).
- [6] H. Sanada et al., Phys. Rev. Lett. 94, 097601 (2005).
- [7] J. M. Kikkawa and D. D. Awschalom, Science 287, 473 (2000).
- [8] G. Salis et al., Phys. Rev. Lett. 86, 2677 (2001).
- [9] Optical Orientation, edited by F. Meier and B.P. Zakharchenya (Elsevier, Amsterdam, 1984).
- [10] M. Eickhoff and D. Suter, J. Magn. Reson. 166, 69 (2004).
- [11] H. Sanada et al., Phys. Rev. Lett. 96, 067602 (2006).
- [12] Y. Hirayama et al., J. Phys. Condens. Matter 18, S885 (2006).
- [13] H. Kampermann and W. S. Veeman, Quant. Info. Proc. 1, 327 (2002).
- [14] We noticed the reduction of coherence times over months together with the increase of quadrupole splittings. This is most probably due to the change in strain in the sample.
- [15] G. Salis, D. D. Awschalom, Y. Ohno, and H. Ohno, Phys. Rev. B 64, 195304 (2001).
- [16] F. A. Bonk et al., Phys. Rev. A 69, 042322 (2004).
- [17] H. Kampermann and W. S. Veeman, J. Chem. Phys. 122, 214108 (2005).
- [18] M. N. Leuenberger and D. Loss, Nature (London) 410, 789 (2001).
- [19] J. M. Taylor, C. M. Marcus, and M. D. Lukin, Phys. Rev. Lett. 90, 206803 (2003).